

## Electronic Supplementary Information

### 1. Materials and Methods

#### 1.1 Materials

Biocoal A was provided by SunCoal Industries GmbH. The rather dry coal (water content 3.2 wt.-% as received) was stored in containers sealed with Parafilm® in the dark. Biocoal B was provided by SmartCarbon AG and dried at 333 K for 24 h to obtain a similar moisture level to Biocoal A which was already dried during the producing CarboREN process (4). Both biocoals were crushed and sieved to a particle size  $\leq 200 \mu\text{m}$  before analytics and reactions. Tetralin (1,2,3,4-tetrahydronaphthalene, purity 97 %) was purchased from Merck. *n*-Pentane (purity 98 %) and nickel(II)nitrate hexahydrate (purity  $\geq 98.5$  %) were purchased from Sigma-Aldrich. Ethoxybenzene (purity  $\geq 99$  %) was obtained by Acros Organics. Aeroxide TiO<sub>2</sub> P90 (fumed titania) was obtained from Evonik. Nitrogen (5.0) and hydrogen (5.0) were purchased from Westfalen.

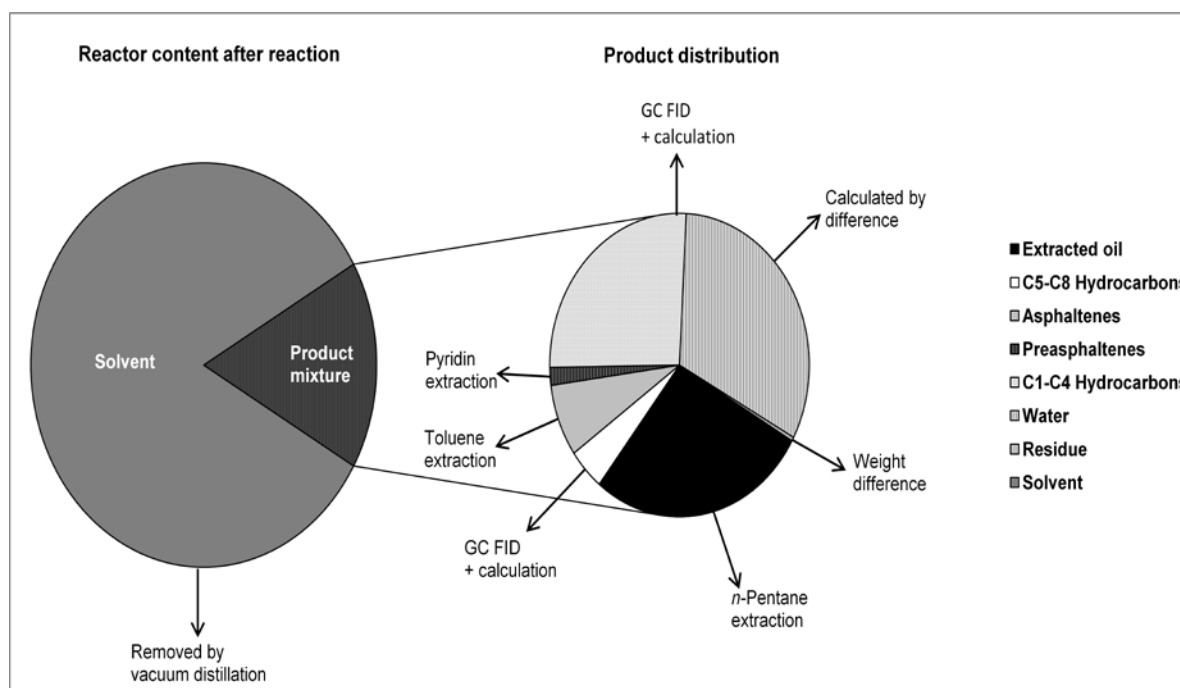
#### 1.2 Catalyst preparation

The Ni/TiO<sub>2</sub> catalyst was prepared by incipient wetness impregnation of aqueous nickel nitrate solution onto fumed titania. Our procedure is a modification the one of Olcese et al.<sup>1</sup>. After impregnation, the catalyst precursor was dried at 393 K over night and calcined at 773 K for one hour (heating rate = 5 K min<sup>-1</sup>) under air flow (100 dm<sup>3</sup> h<sup>-1</sup>). The reduction to elemental nickel on the support was carried out in a quartz glass tube with a temperature of 843 K for 1 h (heating rate 5 K min<sup>-1</sup>) with a hydrogen flow rate of 100 cm<sup>3</sup> min<sup>-1</sup>.

#### 1.3 Direct biocoal liquefaction

Biocoal (10 g, maf), tetralin (50 g, 378.8 mmol) and 18Ni/TiO<sub>2</sub> (1 g,  $m_{\text{Ni}}/m_{\text{maf coal}} = 1.8$  wt.-%, particle size  $\leq 200 \mu\text{m}$ ) were added to a 168 ml high pressure resistant glass inlet. The glass inlet was placed in a 250 ml steel batch autoclave which was assembled on the reactor head. The reactor was purged several times with nitrogen and hydrogen before 10 MPa hydrogen were charged into the reactor while the stirrer was rotated with 5 Hz. The autoclave was heated with a heating jacket to 673 K (heating rate  $\approx 5$  K min<sup>-1</sup>). This was the reaction temperature which was kept for 2 h. The reaction was ended by removing the heating jacket and cooling down to room temperature. The gas phase was collected when the reactor was cooled to 343 K to determine the composition of the organic phase, especially the amount of C<sub>5</sub>-C<sub>8</sub> hydrocarbons, which are difficult to separate with the following distillation, and these hydrocarbons are sufficiently abundant in the gas phase at this temperature. After opening the reactor, the catalysts were separated by a bar magnet (for the exact procedure see 1.4). The liquids and solid residues were collected with acetone. Tetralin was removed by vacuum distillation. The mass balance of the solvent could be closed successfully. After the distillation, the oil products were extracted from the residues by stirring in 100 dm<sup>3</sup> *n*-pentane several times overnight. For the solid residues, thermogravimetric analysis was used to determine the organic fraction (Section 2.4). With known masses of oils (and their composition by elemental analysis, Section 2.3) and organic residues, the mass of the gas phase can be calculated by difference from the original maf coal mass (Scheme S1). The amount of C<sub>5</sub>-C<sub>8</sub> hydrocarbons was calculated under the simplification that the solid residues (which also contain asphaltenes and preasphaltenes) are unconverted coal. This is a pessimistic approximation, since for the

actual conversion preasphaltenes and asphaltenes were included into the amount of converted coal mass. The masses of asphaltenes (soluble in toluene) and preasphaltenes (soluble in pyridine) were determined by soxhlet extraction with toluene and pyridine, respectively, for 3 days followed by drying under vacuum for 3 days at 383 K. The yield of C<sub>5</sub>-C<sub>8</sub> components from the first gas phase analytics were added to the oil yield of the heavier oils from the extraction so that the term gas phase only comprises organic C<sub>1</sub>-C<sub>4</sub> gases and inorganic H<sub>2</sub>O and H<sub>2</sub>S (denoted as inorganic gases, see also Section 2.3). It has been reported before that after heteroelement removal oxygen and sulfur exist as H<sub>2</sub>O and H<sub>2</sub>S under reaction conditions<sup>2</sup>. The reproducibility of the liquefaction experiments was checked with the masses of the extracted oils. The standard deviation of our values for the oil yield was ±0.3 wt.-% for repeated reactions.



**Scheme S1.** Graphical illustration of mass balances.

## 1.4 Catalyst recovery experiments

Spent catalyst was separated by a bar magnet after reaction. The recovered material was rinsed with acetone, dried, and carbonaceous deposits were burnt off at 823 K for 1 h (heating rate 20 K min<sup>-1</sup>) in an air flow of 100 cm<sup>3</sup> min<sup>-1</sup>. The titania-supported nickel oxide particles were reactivated by the same procedure as described in 1.2. Residual ash particles could be separated by further application of a magnetic gradient.

## 2. Characterization and Analytics

### 2.1 Attenuated total reflectance infrared spectroscopy (ATR)

ATR studies were conducted on a Nicolet 6700 FT-IR spectrometer from THERMO scientific company. After a background had been recorded, the coal was fixed on a diamond crystal. The reflection measurements were recorded with 64 scans ranging from 650 to 4000 cm<sup>-1</sup>.

## 2.2 Brunauer-Emmett-Teller (BET) physisorption measurements

Nitrogen physisorption (BET) with a Quantachrome Autosorb 3B was conducted to calculate the specific surface area of catalysts and supports. The nonporous aeroxide TiO<sub>2</sub> P90 support (fumed TiO<sub>2</sub>) had a specific surface area of 80 m<sup>2</sup> g<sup>-1</sup>. The 18Ni/TiO<sub>2</sub> catalyst had a specific surface area of 60 m<sup>2</sup> g<sup>-1</sup>.

## 2.3 CHNS elemental analysis

Carbon, hydrogen and nitrogen were analyzed by an Elemental Analyzer – Mod. 1106 from Carlo Erba. The oxidized sulfur of the burnt organic material was absorbed in a diluted hydrogen peroxide solution and determined quantitatively by titration. When the composition of oil and gas phase (Section 2.4) is known, the mass contents of oxygen and sulfur in the total gas phase as H<sub>2</sub>O and H<sub>2</sub>S can be calculated and subtracted from the total gas phase to receive the mass of the organic gas phase. The C<sub>5</sub>-C<sub>8</sub> contents of the gas phase taken after cooling the reaction mixture to 343 K determined by GC-MS (Section 2.4) are subtracted from the organic gas phase and added to the oil yields since they are considered to be liquids. Thus, it can be assumed that the organic gas phase only contains C<sub>1</sub>-C<sub>4</sub> gases.

## 2.4 GC-MS analytics of organic products

For direct coal liquefaction, the gas phase composition was analyzed by Agilent Technologies 6890N Network GC System. The column Supelco PetrocolDH150 (150 m x 0.25 mm x 1 μm) was used with a flame ionization detector. The gas phase samples were injected manually (100 μl). Detected peaks were assigned by mass spectrometry. Quantitative evaluation of the peak areas was accomplished by the normalization method. Therefore, substance specific correction factors were calculated by a method from Leibnitz and Struppe<sup>3</sup>. The mass fractions calculated from the peak areas were multiplied with the mass of the gas phase to obtain the mass of the respective component. For GC-MS analysis, Agilent 5975 B inlet XL MSD was used.

## 2.5 Inductively coupled plasma-optical emission spectrometry (ICP-OES)

Nickel loadings of the catalyst were determined by dissolving the catalyst in a diluted mixture of hydrofluoric acid, nitric acid and hydrochloric acid followed by digestion in a Berghof Speedwave microwave. The quantitative determination of nickel was achieved via Vista MPX CCD Simultaneous ICP-OES. For the exact metal loadings, water in catalysts was determined by TGA (Section 2.7). For the Ni/TiO<sub>2</sub> catalyst, the nickel loading was 18.2 wt.-% referred to the dry catalyst.

## 2.6 <sup>13</sup>C Crosspolarization MAS-NMR

As complementary structural investigations to ATR (Section 2.1), <sup>13</sup>C CP-MAS-NMR spectra were recorded for the biocoals according to Haenel et al.<sup>4</sup>. A Bruker ADVANCEIII 400WB NMR spectrometer was used for crosspolarization experiments whereby the <sup>1</sup>H nuclei were excited over a frequency of 400.13 MHz and the <sup>13</sup>C nuclei over 100.62 MHz. The pulse duration was 2 ms.

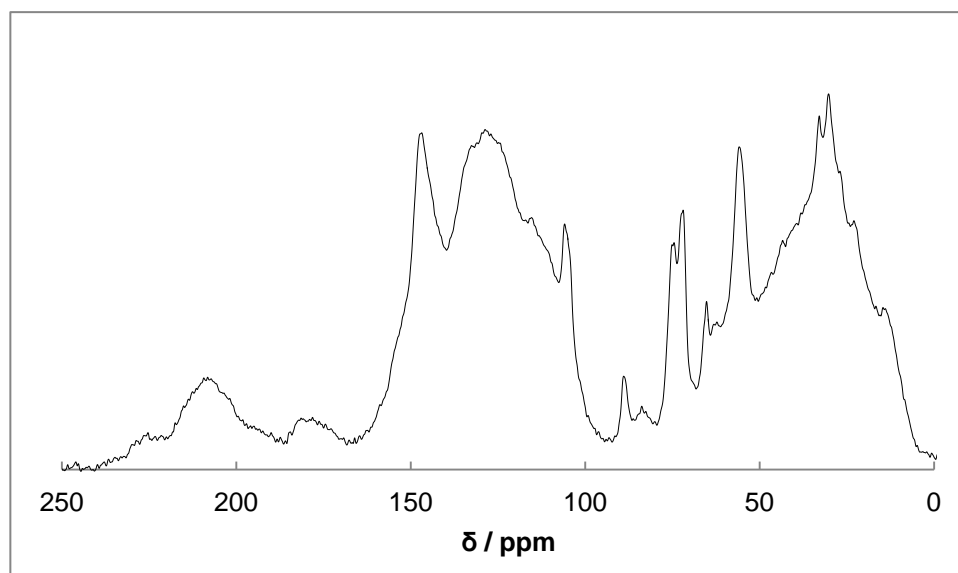


**Fig. S1a.**  $^{13}\text{C}$  MAS-NMR spectrum of Biocoal B.

The spectra of coals can generally be divided into two chemical regions: aliphatic carbons (0-90 ppm) and aromatic carbons (90-220 ppm, including carbonyl/carboxyl and phenolic groups)<sup>5</sup>. The structural findings in NMR widely agree with the findings of functional groups done by ATR (see Section 2.1). Biocoals A and B both have signals at  $\delta = 205$  and 176 ppm (Figures S1a and S1b) which can be assigned to C=O and carboxyl, esters or quinone respectively<sup>5</sup>. The signals at 147 ppm (Biocoal B) and 156 ppm (Biocoal A) are in the range of aromatic ethers or hydroxyls<sup>6</sup>. The broad signals around 125 ppm clearly show the chemical shifts of aromatic C-H or aromatic quaternary carbon<sup>5,6</sup>. The spectrum of Biocoal B shows peaks at 89, 85, 75, 72 and 55 ppm clearly resulting from aliphatic C-O bonds<sup>5,6</sup>. Both biocoal spectra show the most intensive peak at around 30 ppm, which corresponds to  $\text{CH}_2$ , whereby shoulders at around 25 ppm clearly show  $\text{CH}_3$ <sup>5,6</sup>.

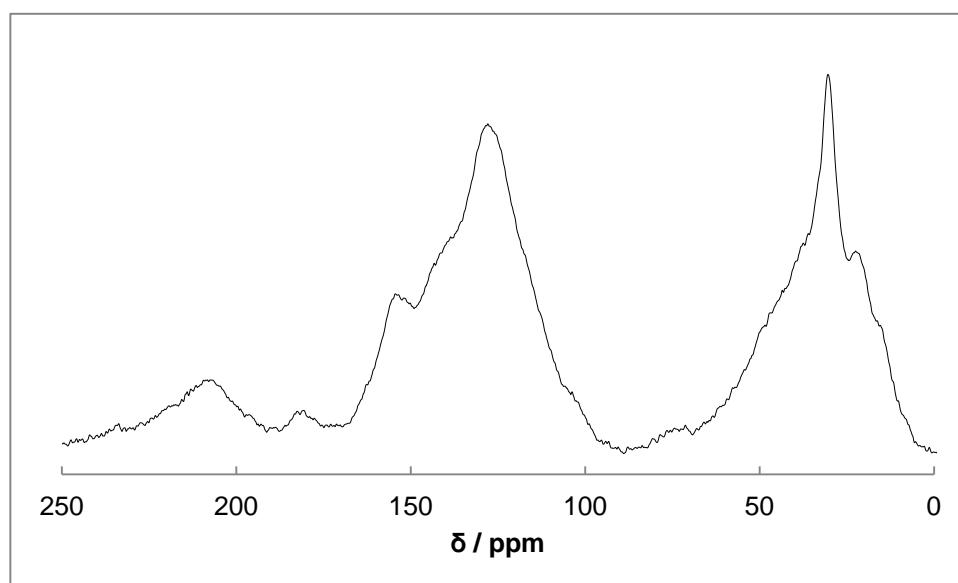


**Fig. S1b.**  $^{13}\text{C}$  MAS-NMR spectrum of Biocoal A.

## 2.7 Thermogravimetric analysis (TGA)

TGA was performed with Setaram Setsys TG 16/18. For the determination of ash and moisture in coal and liquefaction residues, heating programs described in ASTM D-3173 and ASTM D-3174 were used<sup>7</sup>. Water contents of catalysts were determined by heating the material from 293 to 873 K in nitrogen atmosphere (heating rate 20 K min<sup>-1</sup>).

## 2.8 X-ray diffraction (XRD)

Powder XRD (Figure S2) was performed on a Bruker AXD D8 Diffractometer using Cu (K $\alpha$ )-radiation (0.1506 nm, 40 kV, 40 mA). Peak assignments were accomplished by using diffraction patterns of Software DiffracPlus EVA which is correlated with the International Centre for Diffraction Data (ICDD). The reference pattern number for the Ni/TiO<sub>2</sub> assignment is 00-004-0850 for nickel and for the titania support consisting mainly out of anatase phase (00-021-1272) and a little bit of rutile (00-021-1276).

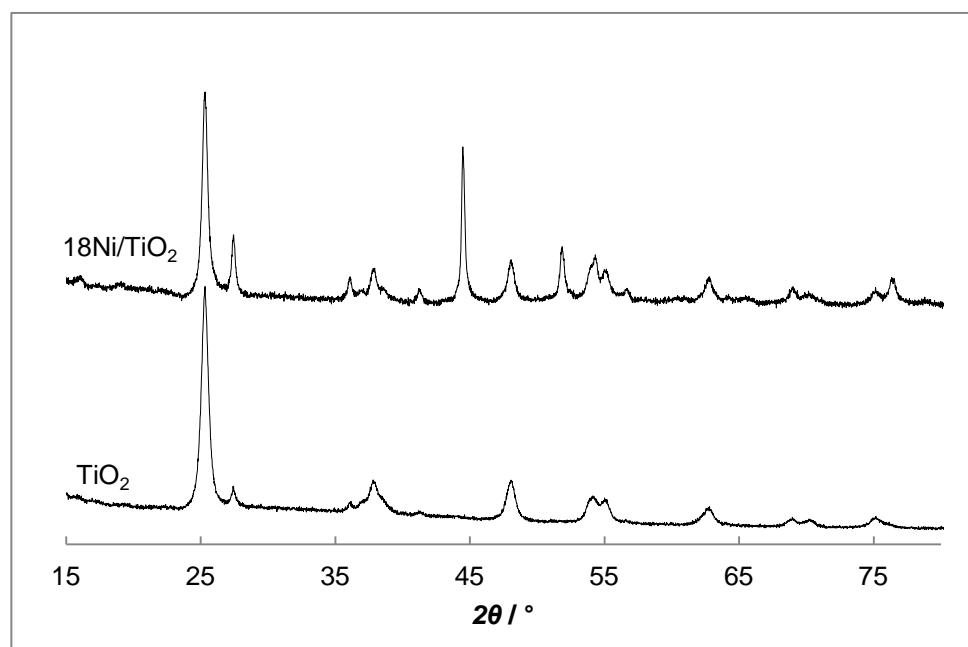


Fig. S2. X-ray powder diffractograms of 18Ni/TiO<sub>2</sub> and TiO<sub>2</sub>.

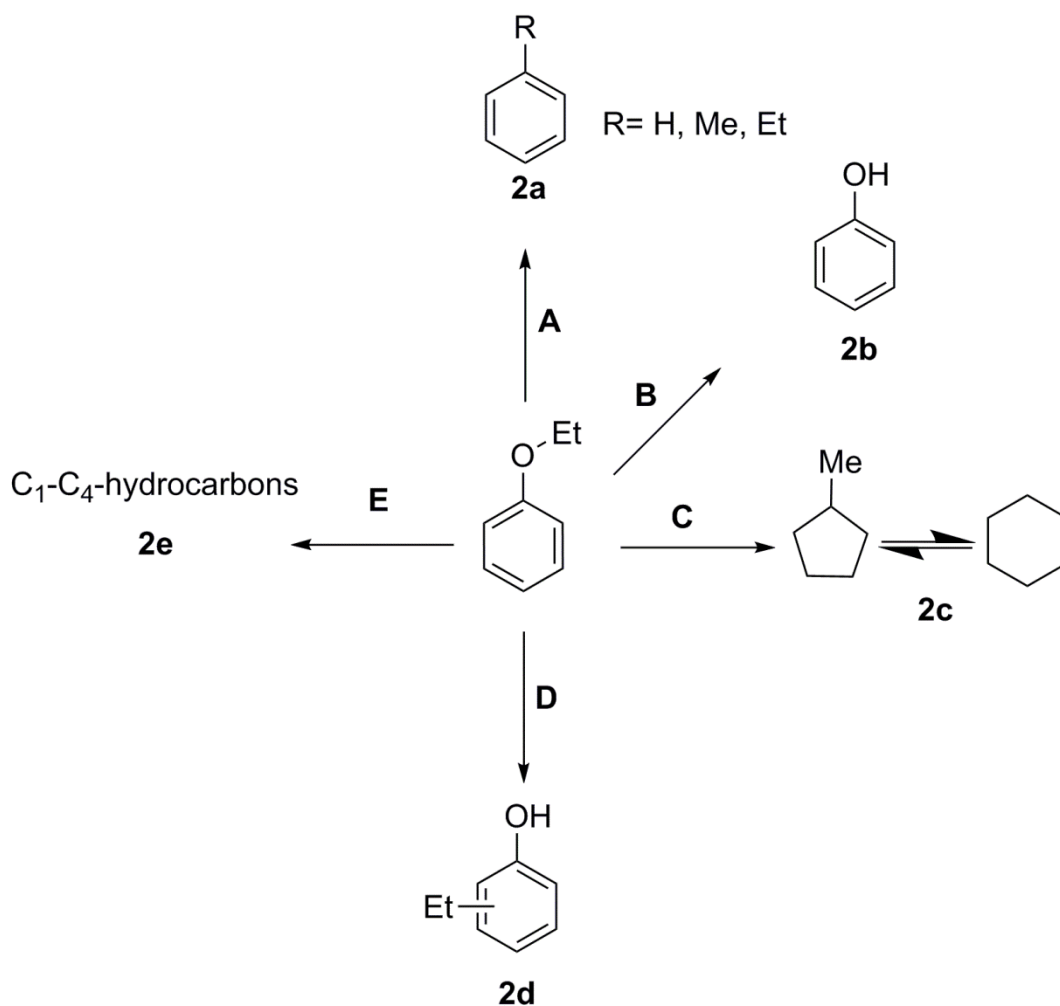
## 2.9 Model compound reactions

For mechanistic investigations coal-related model compounds (CRMCs) can be used. CRMC reactions provide further knowledge about bond-breaking mechanisms in direct coal liquefaction, by using smaller molecules which represent important units of the coal structure. Since the organic structure of both biocoals used encompasses many C<sub>aromatic</sub>-O and C<sub>aliphatic</sub>-O bonds (see sections 2.1 and 2.6), ethoxybenzene was used as CRMC. Besides the replacement of the biocoal by ethoxybenzene (10.0 g, 81.9 mmol) and reducing the reaction time to 1 h, the reaction procedure remained the same as shown in section 1.3. For advanced reaction analysis the liquid phase was collected, weighed and 10  $\mu$ l of the reaction mixture were injected into GC-MS (described in section 2.4). The quantitative composition of the liquid phase was calculated by the corrected FID peak areas and the components of the reaction mixture were identified by MS. The conversion of ethoxybenzene and the product selectivities were calculated according to equations (1) and (2):

$$X_{\text{Etb}} = \frac{n_{\text{Etb},0} - n_{\text{Etb}}}{n_{\text{Etb},0}} \quad (1)$$

$$S_j = \frac{n_j}{n_{\text{Etb},0} - n_{\text{Etb}}} \quad (2)$$

$X_{\text{Etb}}$  stands for the conversion of ethoxybenzene,  $n_{\text{Etb},0}$  is the amount of ethoxybenzene before and  $n_{\text{Etb}}$  is its amount after the reaction (both in moles).  $S_j$  describes the product selectivity for the conversion of ethoxybenzene and  $n_j$  the molar amount of the product. Scheme S2 shows the possible CRMC reactions and products. Reaction **A** is a hydrogenolytic cleavage of the  $\text{C}_{\text{aromatic}}\text{-O}$  bond occurring either thermally, catalytically or by solvent-mediated hydrogenolysis<sup>2</sup> to benzene, toluene or ethylbenzene (BTE) **2a**, and for  $\neq\text{RH}$  an intramolecular transalkylation. The second pathway **B** yields phenol **2b** by hydrogenolytic cleavage of the weaker  $\text{C}_{\text{aliphatic}}\text{-O}$  bond. Reaction **C** is the hydrogenolysis of the ethoxygroup followed by the complete hydrogenation of benzene to **2c**. For this product a equilibrium between methylcyclopentane and cyclohexane is likely, whereby the equilibrium is clearly shifted in favor of cyclohexane. Reaction path **D** can be defined as intramolecular transalkylation to ethylphenol **2d**.  $\text{C}_1\text{-C}_4$  hydrocarbons **2e** are likely to be thermodynamic products appearing over **E** which is a consecutive radical reaction or total hydrogenolysis of the products before.



**Scheme S2.** Reaction network and products for the reaction with the CRMC ethoxybenzene. For simplification only the reactions and products occurring with the aromatic ring are shown.

**Table S1.** Conversions and selectivities of the ethoxybenzene reaction<sup>a</sup>.

Catalyst	$X_{\text{Etb}} / \%$	$S_{2a} / \%$	$S_{2b} / \%$	$S_{2c} / \%$	$S_{2d} / \%$	$S_{2e} / \%$
-	57	19	46	0 <sup>[b]</sup>	6	29
TiO <sub>2</sub> <sup>[c]</sup>	92	5	40	0 <sup>[b]</sup>	29	26
18Ni/TiO <sub>2</sub>	80	11	34	11	13	31

<sup>a</sup> Reaction conditions: 10 MPa H<sub>2</sub> initial pressure,  $m_{\text{ethoxybenzene}} = 10.0$  g (81.9 mmol),  $m_{\text{tetralin}} = 50.0$  g (378.8 mmol),  $m_{18\text{Ni}/\text{TiO}_2} = 1$  g,  $T_{\text{reaction}} = 673$  K,  $t_{\text{reaction}} = 1$  h. <sup>b</sup> Not detected. <sup>c</sup>  $m_{\text{TiO}_2} = 0.82$  g.

The product selectivities  $S_j$  and the CRMC conversions are shown in Table S1. The ethoxybenzene conversions are clearly higher for the catalytic reactions with TiO<sub>2</sub> (92 %) and 18Ni/TiO<sub>2</sub> (80 %) than without a catalyst (57 %). In the latter case, the reactions either take place thermally or by the solvent. Mainly the cleavage of C<sub>aliphatic</sub>-O bond **B** occurs ( $S_{2b} = 46$  %) since its bond dissociation energy (339 kJ mol<sup>-1</sup>) is clearly smaller than that of the C<sub>aromatic</sub>-O bond (422 kJ mol<sup>-1</sup>)<sup>8</sup>. This fact is proved by the smaller selectivity  $S_{2a} = 19$  % for reaction **A**. Product **2b** is very stable since the bond dissociation energy for C<sub>aliphatic</sub>-OH (468 kJ mol<sup>-1</sup>) is higher than for ethers shown above<sup>8</sup>. When the support TiO<sub>2</sub> is used as a catalyst, the selectivity for **2a** significantly drops to 5 %, although the conversion is much higher. This observation is owed to the higher selectivity for **2d** (29 %) which is formed by intramolecular transalkylation **D** catalysed by the TiO<sub>2</sub> support which is obviously faster than the temperature- or solvent-induced cleavage of C<sub>aromatic</sub>-O. The reason for this behavior are the hydroxylic surface functionalities, mainly bridging hydroxyl groups of TiO<sub>2</sub>, which act as Brønsted acids<sup>9</sup>. Strassberger *et al.* could report a similar behavior for the intramolecular transalkylation of ethoxybenzene by using Al<sub>2</sub>O<sub>3</sub> as a catalyst which also has an acidic surface<sup>10</sup>.

When 18Ni/TiO<sub>2</sub> is used as a catalyst, the conversion drops to 80 % and the selectivity for product **2d** decreases to 13 %. The selectivity to **2a** increases to 11 % and the selectivity for **2c** over hydrogenation **C** is 13 %. The decreases of  $X_{\text{Etb}}$  and  $S_{2d}$  in contrast to the reaction with TiO<sub>2</sub> only can be explained by the high nickel loading, which blocks the acidic centers of TiO<sub>2</sub>. This is in line with the work of Strassberger *et al.*, who reported for Al<sub>2</sub>O<sub>3</sub> that the selectivity for the intramolecular transalkylation is strongly reduced by addition of MgO<sup>10</sup>. In this case the activation of hydrogen by metallic nickel clearly increased the selectivity for hydrogenation of the aromatic ring **C**.

If those results are applied to the mechanism of the direct biocoal liquefaction, it becomes clear, why noncatalytic runs including only thermal and solvent reactions, mainly generating the scission of weak C<sub>aliphatic</sub>-O linkages, have lower conversions (78 %) and lower oil yields (17 wt.-%) for Biocoal A. This is accompanied by poorer oil characteristics, namely a lower molar H/C ratio (1.16) and a higher oxygen content (7.0 wt.-%) leading to a worse *HHV* (39.5 MJ kg<sup>-1</sup>) than for the catalytic run with 18Ni/TiO<sub>2</sub> ( $X_{\text{coal}} = 99$  %,  $HHV_{\text{oil}} = 41.0$  MJ kg<sup>-1</sup>, H/C molar ratio = 1.32,  $Y_{\text{oil}} = 32$  wt.-%). The catalyst can break strong C<sub>aromatic</sub>-O bonds in the biocoal leading to higher conversions and higher oil yields and a smaller oxygen content in the product oil (4.6 wt.-%). Additionally, the oil quality is improved because of the hydrogenation activity for aromatic rings. Due to the activity of the titania support for intramolecular transalkylation of alkoxyaromatics, smaller fragments like for example methyl or ethyl remain in the product oil since they are connected to an aromatic ring and are not eliminated as gas phase products like for example methane or ethane.

## 2.10 Further oil analytics

The product oil from the direct biocoal liquefaction is composed of a light biooil, obtained from the gas phase, which is 5 wt.-% out of the 32 wt.-% total oil yield from Biocoal A and 4 wt.-% out of the total oil yield (36 wt.-%) from Biocoal B. The other 27 respectively 32 wt.-% of the total biooil products which can be extracted by *n*-pentane are called extracted biooils. The composition of the biooil extracted from Biocoal A is 85.9 wt.-% carbon, 8.6 wt.-% hydrogen, 0.3 wt.-% nitrogen and 5.2 wt.-% oxygen and for the oil extracted from Biocoal B 84.9 wt.-% carbon, 8.4 wt.-% hydrogen, 2.1 wt.-% nitrogen and 4.6 wt.-% oxygen. The extracted biooils, dark brown liquids, are not sufficiently vaporizable for GC-MS analytics, so the only further characterization was done by ATR (see Manuscript Figure 3). The composition of the light oils from both biocoals is shown in Figure S3. The product distributions for the light biooils are similar for both liquefied biocoals. The light biooil mainly consist of *n*-alkanes, *iso*-alkanes and cycloalkanes in the major abundant C<sub>5</sub>-C<sub>6</sub> fractions. The C<sub>7</sub>-C<sub>8</sub> fractions are mainly open-chain aliphatics. By contrast, the extracted oils have a stronger aromatic character (see Fig. 3 in the manuscript) which is concordant with the molar H/C ratios.

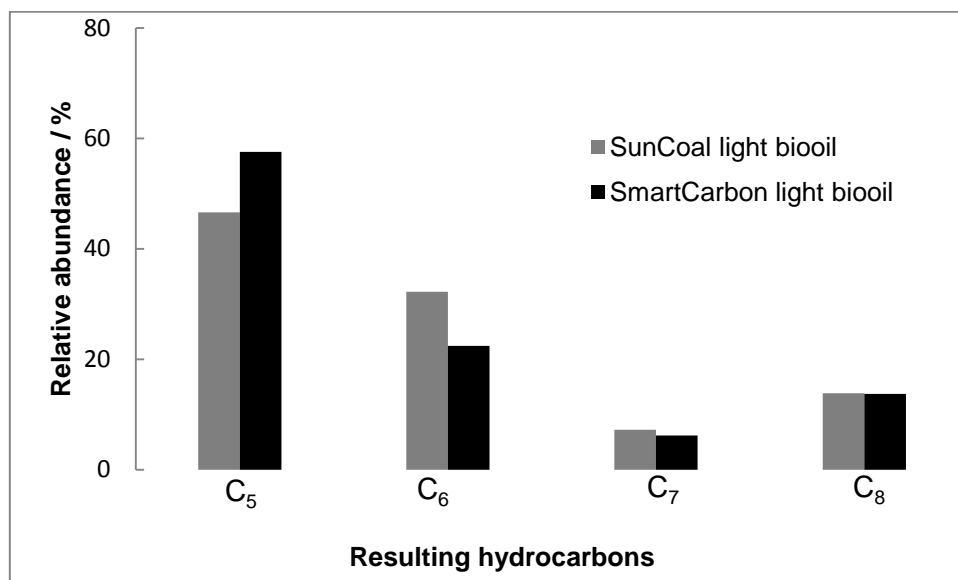


Fig. S3. Composition of the light oil fractions from both direct biocoal liquefaction reactions.

## 2.11 Hydrogen chemisorption

H<sub>2</sub> chemisorption measurements were conducted on a Quantachrome Autosorb-1 instrument at 318 K. The samples were pretreated at 623 K under H<sub>2</sub> flow for 1h (heating rate 5 K min<sup>-1</sup>).



### 3. References

- 1 R.N. Olcese, M. Bettahar, D. Petitjean, B. Malaman, F. Giovanella, A. Dufour, *Appl. Catal., B*, 2012, **115-116**, 63.
- 2 S. Vasireddy, B. Morreale, A. Cugini, C. Song, J.J. Spivey, *Energy Environ. Sci.*, 2011, **4**, 311.
- 3 T. Kratzsch, in *Handbuch der Gaschromatographie*, ed. E. Leibnitz, H.G. Struppe, Akademische Verlagsgesellschaft Geest&Portig K.-G., Leipzig, 3rd ed., 1984, pp. 405-439.
- 4 a) M.W. Haenel, J. Narangerel, U.-B. Richter, A. Rufinska, *Angew. Chem. Int. Ed.*, 2006, **45**, 1061; b) M.W. Haenel, J. Narangerel, U.-B. Richter, A. Rufinska, *Angew. Chem.*, 2006, **118**, 1077.
- 5 M. Hesse, B. Meier, M. Zeeh, in *Spektroskopische Methoden in der organischen Chemie*, ed.: M. Hesse, B. Meier, M. Zeeh), Thieme Verlag, Stuttgart, 7th ed, 2005, , pp. 1-447.
- 6 B.-O. Erdenetsogt, I. Lee, S.K. Lee, Y.-J. Ko, D. Bat-Erdene, *Int. J. Coal Geol.*, 2010, **82**, 37.
- 7 J. G. Speight, in *Handbook of Coal Analysis*, ed. J. D. Winefordner, Wiley & Sons, New Jersey, 2005, vol. 166, pp. 42-55.
- 8 E. Furimsky, *Appl. Catal., A*, 2000, **199**, 147.
- 9 M. Crocker, R.H.M. Herold, A.E. Wilson, M. Mackay, C.A. Emeis, A.M. Hoogendoorn, *J. Chem. Soc. Faraday Trans.*, 1996, **92**, 2791.
- 10 Z. Strassberger, S. Tanase, G. Rothenberg, *Eur. J. Org. Chem.*, 2011, 5246.